Inorganic Chemistry Communications 176 (2025) 114239

Contents lists available at ScienceDirect

Inorganic Chemistry Communications

journal homepage: www.elsevier.com/locate/inoche

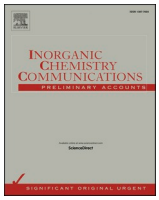

Research Article

In situ synthesis of biocompatible $NaY_{1-x}Gd_xF_4$:Yb/Er nanoparticles for cell labeling and temperature sensing

Miljana Piljević [a], Ivana Dinić [b,*], Lidija Mancic [b], Marina Vuković [b], Miloš Tomić [b], Maria Eugenia Rabanal [c], Miloš Lazarević [d], Mihailo D. Rabasović [a,*]

[a] Photonic Center, Institute of Physics Belgrade, University of Belgrade, Pregrevica 118, Zemun, 11080 Belgrade, Serbia
[b] Institute of Technical Sciences of SASA, Kneza Mihaila 35, 11000 Belgrade, Serbia
[c] Department of Materials Science and Engineering and Chemical Engineering, Universidad Carlos III de Madrid and IAAB, 28903 Madrid, Spain
[d] School of Dental Medicine, University of Belgrade, Dr Subotica 8, 11000 Belgrade, Serbia

ARTICLE INFO

Keywords:
$NaY_{1-x}Gd_xF_4$:Yb/Er
Nanoparticles
Upconversion luminescence
Temperature sensing
Cell labeling

ABSTRACT

Biocompatible, up-converting $NaY_{1-x}Gd_xF_4$:Yb/Er nanoparticles have been successfully obtained *in situ* by chitosan assisted solvothermal synthesis, and were further characterized to check their potential for optical thermometry. The temperature dependent change in the green emission intensity, originating from the thermalization between $^4S_{3/2}$ and $^2H_{11/2}$ levels, implied maximum relative sensitivity of 1.3 $\%K^{-1}$ in the physiologically interesting temperature range. Presence of chitosan ligands at the nanoparticles surface promotes their biocompatibility. The nanoparticles concentration ranging from 10 to 50 μg/mL yielded viability higher than 80 % for HS-5 fibroblast and SCC-25 oral cancer cells. Efficient visualization of $\alpha NaY_{0.65}Gd_{0.15}F_4$:$Yb_{0.18}Er_{0.02}$ nanoparticles in cytoplasmic region of cells, under excitation at 976 nm, validates their potential to be used for cell labeling and temperature sensing in tissue.

1. Introduction

Rare earth (RE) doped up-converting nanoparticles (UCNPs) represent a light emitting material. Its optical activity results from the presence of dopants that allow up-conversion (anti-Stokes) emission, a nonlinear optical process of absorbing two or more low-energy photons and emitting photon which energy is higher than its excitation counterparts [1–3]. The optical properties of UCNPs come from the unique electronic configuration of RE^{3+} ions, in which the $4f^N$ orbital is shielded from the chemical environment by the outermost $5s^2$ and $5p^6$ orbitals, so f-f transitions raised from the $^{2S+1}L_J$ sublevels are partially allowed [4,5]. The intensity of the emission lines depends on the type of electronic transition established, which in turn depends on structural characteristics of UCNPs. Because of their lowest phonon lattice energy (~350 cm^{-1}), fluorides have proven to be the most suitable host materials for RE^{3+} doping, when compared to other inorganic materials [6,7]. Among them, the hexagonal $NaYF_4$ and orthorhombic YF_3 have a much higher emission intensity than cubic $NaYF_4$ phase, due to fact that later possess more symmetrical crystal structure [8,9]. This is exploited for many applications in optoelectronics, lightening and solar energy harvesting. Nevertheless, RE^{3+} doped fluorides also received considerable attention in medicine as new cell labels, and drug delivery agents, because when doped with Nd^{3+} or Yb^{3+} (as sensitizer), and co-doped with Er^{3+}, Ho^{3+}, or Tm^{3+} (as activator), these could be excited by the wavelengths from the first and second near-infrared (NIR) biological windows where light has its maximum depth of penetration in tissue, and minimum interaction with the tissue components [2,3,10]. Furthermore, it is shown that their temperature-sensing behavior, based on the luminescence intensity ratio (*LIR*) from the thermally coupled levels of activator ions, could be used for non-invasive remote sensing of temperature. To date, beside to the most advantageous hexagonal $NaYF_4$:Yb/Er phase, RE-doped $NaGdF_4$, YF_3, $Y_6O_5F_8$, and $Ba_3Gd_2F_{12}$ are explored for this purpose [11–17].

Various synthesis techniques, including co-precipitation, sol–gel, and hydro/solvothermal processes, along with the application of oleic acid or ligand exchange, have been documented for the synthesis of UCNPs that have controlled crystalline phase composition, size, and morphology, as well as strong luminescent properties [2,18–20]. However, hydrophobic ligand-covered UCNPs produced in this manner need further processing (oxidation or exchange of ligands) for providing

* Corresponding authors.
E-mail addresses: ivana.dinic@itn.sanu.ac.rs (I. Dinić), rabasovic@ipb.ac.rs (M.D. Rabasović).

https://doi.org/10.1016/j.inoche.2025.114239
Received 7 February 2025; Received in revised form 26 February 2025; Accepted 2 March 2025
Available online 4 March 2025

biocompatibility and water dispersibility [21]. Alternatively, biocompatible capping ligands such as polyethyleneimine (PEI), dibenzoic acid (DBA) and trisodium citrate (TSC) were successfully used during synthesis of various hybrid structures [3,22,23]. Besides these, chitosan (CS) is also considered an important biopolymer for medical and pharmaceutical applications, especially for encapsulation of magnetic carriers, controlled drug delivery, wound dressings, and tissue engineering [24,25]. The inter-dispersed acetamido groups of CS increase its biocompatibility, biodegradability, reactivity, non-toxicity, antifungal and antimicrobial activity [26,27].

In our earlier research, we reported for the first time that addition of chitosan during the hydro/solvothermal synthesis of cubic $NaYF_4$:Yb/Er provides generation of UCNPs with adequate hydrophilicity and amino-functionalized surface, without compromising the luminescence [28]. Here, a similar synthesis approach is used for *in situ* obtaining biocompatible $NaY_{1-x}Gd_xF_3$:Yb/Er nanoparticles. Due to fact that Er^{3+} is the most commonly used RE^{3+} ion for optical thermometry, *LIR*-based temperature sensitivity originating from the thermally coupled $^2H_{11/2}$ and $^4S_{3/2}$ energy levels, NIR-cell imaging, and cytotoxicity of the UCNPs were investigated.

2. Materials and methods

All of the chemicals used for chitosan assisted solvothermal synthesis of $NaY_{0.8}F_4$:$Yb_{0.18}Er_{0.02}$ (S1) and $NaY_{0.65}Gd_{0.15}F_4$:$Yb_{0.18}Er_{0.02}$ (S2) UCNPs were purchased from Sigma-Aldrich: $Y(NO_3)_3{\cdot}6H_2O$, $Gd(NO_3)_3{\cdot}6H_2O$, $Yb(NO_3)_3{\cdot}5H_2O$ and $Er(NO_3)_3{\cdot}5H_2O$, NaF, $C_2H_6O_2$, and $C_{56}H_{103}N_9O_{39}$ (CS: 50,000–190,000 Da). Deionized water was used throughout. Defined stoichiometric amounts of rare earth nitrates were dissolved in 10 mL of deionized water and mixed with 15 mL of chitosan solution (0.3 mmol/L). Then, 10 mL of NaF solution was added (F^+:RE^{3+} = 14:1). Finally, 35 mL of the ethylene glycol–water (1:1) mixture was added. Obtained precursor solution with final concentration of 2.5 mmol/L was stirred for 20 min and then transferred to a 100 mL Teflon-lined autoclave. The synthesis was performed at 200 °C (4 h) under continuous stirring (100 rpm). After completion of the reaction, obtained precipitate was washed/centrifuged with ethanol and water several times (8000 rpm, 5 min) and dried at 90 °C for 2 h.

The phase composition of the UCNPs was determined by the X-ray powder diffraction (XRPD) using Rigaku Smart Lab diffractometer, equipped with a Cu-Kα source (λ = 1.5406 Å) using a scanning rate of 0.02°/s. The structural data for the powders were acquired through Rietveld refinement in Topas 4.2 (Bruker AXS GmbH, Karlsruhe, Germany) [29]. The morphological features and chemical purity of the particles were investigated by scanning electron microscopy (SEM) coupled energy-dispersive X-ray spectroscopy (EDS), SEM- Philips XL 30/EDAX-Dx4, Amsterdam, Netherlands and transmission electron microscopy (TEM), JEOL JEM 2100. UCNPs structure is additionally confirmed by performing selected area electron diffraction (SAED). The mean size of particles was calculated from SEM images by measuring radius of minimum 200 particles in SemAphore 5.21. Fourier transform infrared spectroscopy (FT-IR) was done on a Nicolet iS10 FT-IR Spectrometer (Thermo Scientific Instruments) in the spectral range from 400 to 4000 cm^{-1}. Photoluminescence (PL) emission measurements were performed at room temperature using a TE-cooled CCD fluorescence spectrometer (Glacier X, BWTEK, Plainsboro, NJ, USA) and 976 nm single mode pigtailed BL976-SAG300 laser diode (Thorlabs, Newton, NJ, USA For temperature-dependent measurements of PL intensity, a PID temperature-controlled plate (Solid State Heat/Cool Plate AHP-1200C21, from TECA, Illinois, USA) was employed in the temperature range from 20 to 65 °C. In order to avoid the local heating of the sample, the excitation was performed via laser radiation in pulses of 100 ms. The luminescent radiation was collected using a multimode optical fiber with a large diameter (0.6 mm) and a large numerical aperture (0.22), and further introduced into the spectrometer. All spectrograms were recorded without pulse averaging and were fitted with 6 separate Gaussian spectral lines, and appropriate integrals were used to find the *LIR*. The stability of the temperature measurement was determined by a series of consecutive measurements performed at 25 and 45 °C. The interval between two consecutive measurements was 2 min at a temperature of 25 °C and 1 min at 45 °C. Ten consecutive measurements were performed so that the total time in which stability was observed was 20 min and 10 min, respectively for 25 °C and 45 °C.

For determination of cytotoxicity and capability of UCNPs to be used for cell labeling, HS-5 (ATCC®, CRL-3611™) and SCC–25 (ATCC®, CRL–1628™) cell lines were used. The cells were cultured in T25 cell culture flasks with a complete growth medium − Dulbecco's Modified Eagle Medium (DMEM) supplemented with 10 % Fetal Bovine Serum (FBS), 100 U/mL of a penicillin–streptomycin solution, and 400 ng/mL hydrocortisone (all chemicals obtained from Invitrogen, Thermo Fisher Scientific, Waltham, MA, USA). The cultivation took place in a humidified atmosphere containing 5 % CO_2 at a temperature of 37 °C. The complete growth medium was replaced every 2–3 days.

To assess cytotoxicity, suspensions of S2 were prepared at three concentrations: 10, 25, and 50 μg/mL. For each concentration, an appropriate mass of S2 was aseptically weighed and suspended in sterile water, followed by vigorous shaking and sonication for 3 min. HS-5 cells, and SCC-25 oral cancer cell lines were seeded in a 96-well plate at a density of 10,000 cells per well and incubated at 37 °C in a humidified atmosphere containing 5 % CO_2. After 24 h, 100 μl of S2 solution was added to each plate at concentrations of 10, 25, or 50 μg/mL. After 24 h of incubation with the cell cultures, the media was discarded, and the cells were washed once with PBS. Subsequently, 100 μL of medium containing 3-(4,5-dimethylthiazol-2-yl)-2,5 diphenyltetrazolium bromide (MTT, 0.5 mg/mL) (Sigma-Aldrich, St. Louis, USA) was added to each well, followed by an additional 4-hour incubation, as previously described by Mancic et al. [30]. The supernatant was removed, and formazan crystals were dissolved in 100 μl of dimethyl sulfoxide (DMSO) (Sigma-Aldrich, St. Louis, USA) by shaking for 20 min at 37 °C. Optical density was assessed at 540 nm utilizing a microplate reader (RT-2100c, Rayto, China). The control group were the cells cultured without S2.

Cell labeling was performed using following protocol: SCC-25 and HS-5 cells were placed at a density of 10^4 cells/cm^2 onto sterile circular glass coverslips with a diameter of 18 mm and incubated for 24 h. After that period, the cells were incubated with 10 μg/mL of S2 solution for another 24 h. The cell then underwent three PBS rinses, followed by fixation with 4 % paraformaldehyde for 20 min. Following fixation, the cells were then mounted with Mowiol (Sigma-Aldrich) onto microscope slides after being washed three times in PBS to remove paraformaldehyde residuals. Samples were stored in the dark at room temperature until imaging.

Two-photon excited (auto)fluorescence of SCC-25 and HS-5 cells and up-conversion response of UCNPs were recorded using a custom-made nonlinear laser scanning microscope with the excitation wavelengths of 730 nm and 976 nm, respectively. Microscope set-up description is given elsewhere [30,31]. The signal was collected in back reflection, using an oil immersion objective lens with high numerical aperture (EC Plan-NEOFLUAR, NA = 1.3; Carl Zeiss AG, Oberkochen, Baden-Wurttemberg, Germany). A visible wide range bandpass filter (390–695 nm, Thorlabs FESH0700) was used to filter out the laser and transmit only the signal. Obtained raw data was processed and analyzed using ImageJ software (1.47v, National Institutes of Health, Bethesda, MD, USA).

3. Results and discussion

In accordance to JCPDS database, $NaYF_4$ phase at ambient pressure and room temperature crystallizes in two crystal forms: a non-stoichiometric cubic (α) *Fm-3m* structure and hexagonal (β) *P63/m* structure, while YF_3 phase crystallizes with the orthorhombic *Pnma* arrangement. The XRPD patterns, Fig. 1, reflect that both samples are

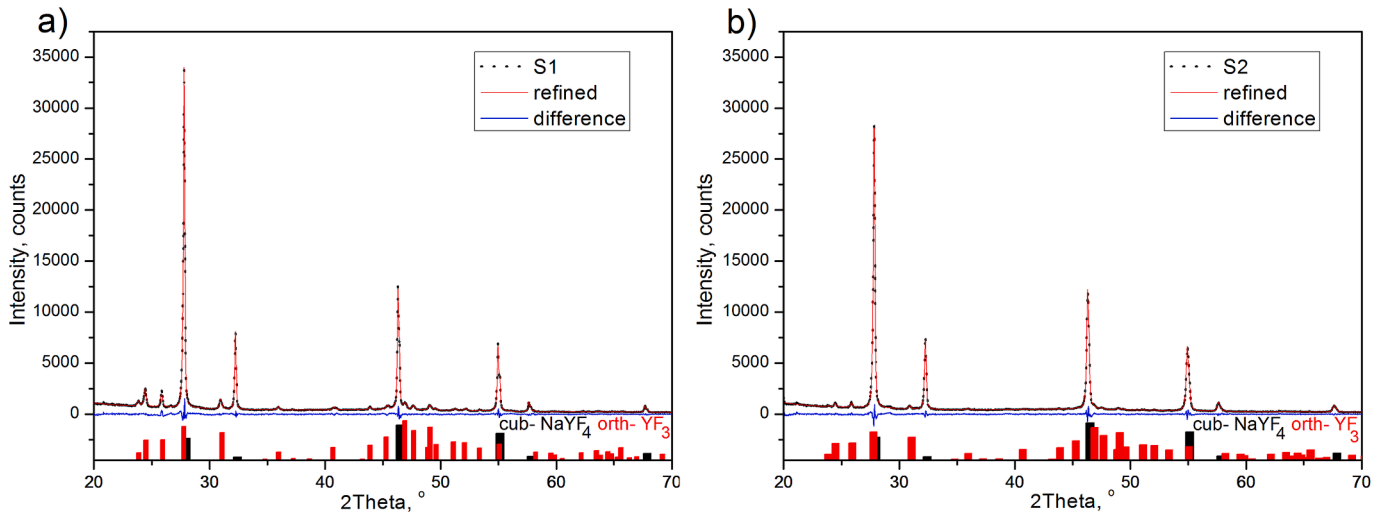

Fig. 1. XRPD data of samples S1 and S2. The experimental data are shown as the black dotted pattern while the red solid line corresponds to the calculated data. The residuals are plotted in the blue line.

composed from cubic α phase (JCPDS 01-77-2042). Minor content of YF_3 phase (JCPDS 01-074-0911), as secondary one is noticeable in both spectra. The sharp and narrow diffraction peaks indicate the good crystallinity of synthetized powders. Based on the XRPD structural refinement, introduction of Gd^{3+} ion (8-fold coordination) with a larger ionic radius (1.053 Å) than Y^{3+} (1.019 Å), led to the slight increase of the crystal lattice parameters and crystal strain in sample S2, Table 1. The weakening of YF_3 reflections in S2 pattern, Fig. 1b, suggests that substitution of gadolinium favors the formation of the single-phase $\alpha NaY_{0.65}Gd_{0.15}F_4{:}Yb_{0.18}Er_{0.02}$, as solid solution.

SEM image of sample S1 shows two distinct particle morphologies that include small spherical particles and larger polyhedrons (Fig. 2a), well consistent with the presence of two phases observed by XRPD. The growth of spherical particles (with a minimized surface energy) typically results in the formation of high packing-fraction structures, such as the *Fm-3 m* face-centered cubic one. Well-defined sub-units, visible at the particles surface, indicate that these are self-assembled of much smaller grains which size is of about few tens of nanometers. Bigger polyhedron-shaped particles with a flat surface are also notable, and these are associated with the orthorhombic YF_3 phase, see Fig. S1. Their content lessens in sample S2, Fig. 2c. Both samples are of high elemental purity, as it is shown in corresponding energy dispersive spectroscopy analysis, Fig. 2b,d. The slight decrease of the mean size of spherical particles (from 257 ± 35 nm in S1 to 200 ± 35 nm in S2) is notable from insets in Fig. 2b,d. In order to check the crystal structure of spherical particles, TEM/HRTEM/SAED analysis of S2 sample is performed, Fig. 3. The clear lattice fringes of (1 1 1) planes (3.158 Å, JCPDS 01-77-2042) visible in Fig. 3c, indicates good crystallinity of spherical $\alpha NaY_{0.65}Gd_{0.15}F_4{:}Yb_{0.18}Er_{0.02}$ nanoparticles, while the SAED spot pattern presented at Fig. 3d implies their mesocrystalline structure.

Table 1
Refined microstructural parameters of UCNPs.

Sample		Unit Cell Parameters (Å)			CS (nm)	Strain	R_{Bragg}
		a	b	C			
S1	Cubic	5.524 (1)	5.524 (1)	5.524 (1)	170 (4)	0.044 (3)	3.3
	Orthorombic	6.332 (1)	6.846 (1)	4.408 (1)	136 (24)	0.200 (5)	3.4
S2	Cubic	5.536 (1)	5.536 (1)	5.536 (1)	162 (7)	0.265 (3)	0.67
	Orthorombic	6.362 (1)	6.868 (1)	4.420 (1)	184 (8)	0.366 (8)	1.4

The preservation of chitosan ligands onto their surface is revealed by the FT-IR analysis, Fig. 4. Based on the spectra obtained, the following chitosan related vibrations are observed in both samples at: 3356 cm^{-1} (stretching vibration of —OH and amine —NH group), 2870 cm^{-1} (C—H bond in $—CH_3$), 1651 cm^{-1}(C═O stretching), 1559 cm^{-1}(NH stretching), 1375 cm^{-1}(CH_3 bending vibrations) and 1051 cm^{-1} (C—O stretching vibration) [32–34]. Comparing with the spectra of commercial chitosan, it may be noticed that in the spectra of S1 and S2 samples, the bands of the —OH (and —NH) and —CH stretching are almost undetectable, while in the 1500–900 cm^{-1} range analogous absorption bands were present. Their weaker intensities and slight shifting from positions in the spectrum of pure chitosan is due to coupling of ligands to the nanoparticles surface.

Fig. 5a shows the normalized up-converting (UC) emission spectra of both samples under 976 nm excitation. The visible emissions detected at 408, 523/548, and 655 nm, which originate from $^2H_{9/2}$, $^2H^4_{11/2}/S_{3/2}$, and $^4F_{9/2}$ to $^4I_{15/2}$, transitions of Er^{3+} ions, define yellowish-green light output for S1: CIE 1931 (0.4416 ± 0.0016; 0.5077 ± 0.0031) and for S2: CIE 1931 (0.4330 ± 0084; 0.5365 ± 0.0080), Fig. 5b. It is known that UC efficiency depends on the ground state absorption (GSA), energy transfer (ET), photon avalanche (PA), cooperative energy transfer (CET), and energy migration-mediated up-conversion (EMU) mechanisms. Simplified energy diagram with a proposed energy transfer processes is presented in Fig. 5c. After absorption of NIR photons, Yb^{3+} ions are excited from the $^2F_{7/2}$ ground state to the $^2F_{5/2}$ excited state and transfer this energy to the $^4I_{11/2}$ state of the Er^{3+} ion. Two possible scenarios can promote the higher excited levels of Er^{3+}. One is through the green-emitting levels ($^4S_{3/2}$ and $^2H_{11/2}$) populating the ^4G,^2K manifold, and the other is through the red-emitting level ($^4F_{9/2}$) populating the level of $^2H_{9/2}$. Non-radiative relaxation from $^4F_{7/2}$ to the $^2H_{11/2}$ and $^4S_{3/2}$ states empowers further radiative de-excitations to the ground $^4I_{15/2}$ state, generating green emission at 523 nm ($^2H_{11/2} \rightarrow {}^4I_{15/2}$) and 548 nm ($^4S_{3/2} \rightarrow {}^4I_{15/2}$). Consecutive absorption of two NIR photons is needed for red emission from $^4F_{9/2}$ level. It could be additionally intensified by the non-radiative $^4F_{7/2}$ relaxation. Blue UC emission from $^2H_{9/2}$ observed at 408 nm is attributed to ET promoting Er^{3+} from $^4F_{9/2}$ up to, or above, the blue-emitting $^2H_{9/2}$ level [17,35–37]. Superior emission of S2 sample observed, could be a consequence of more uniform nanoparticle morphology and phase purity, but also of Gd co-doping effect on of local crystal field asymmetry around emitting Er^{3+} in $\alpha NaY_{0.65}Gd_{0.15}F_4{:}Yb_{0.18}Er_{0.02}$ structure, as it was indicated earlier for this, and other phosphor host materials [38–40].

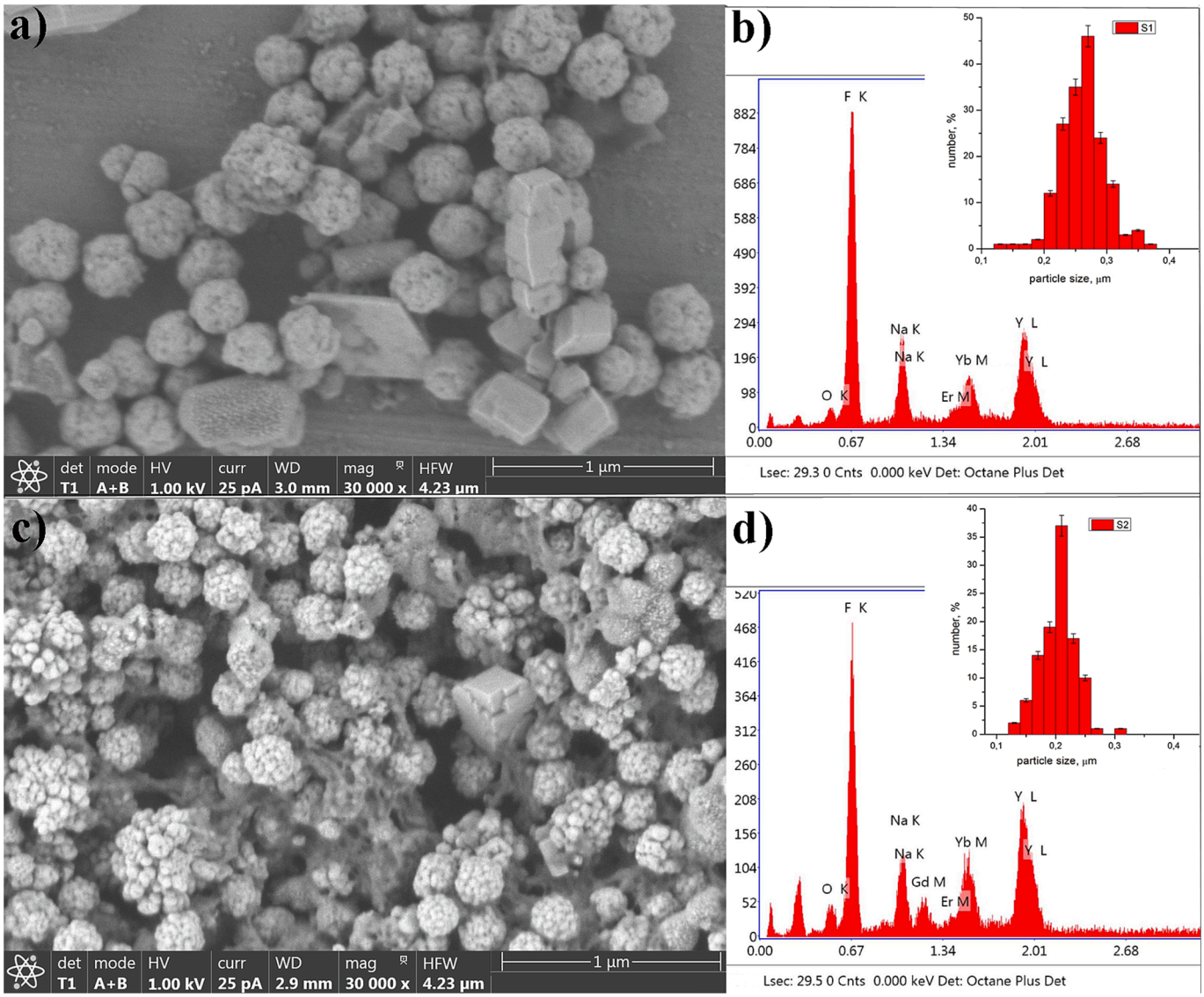

Fig. 2. SEM with corresponding EDS and size distribution of spherical particles in samples S1 (a, b), and S2 (c, d).

To check its bio-compatibility through assessing cytotoxicity, MTT colorimetric assay was performed. Viability of the HS-5 and SCC-25 cells after 24 h incubation with 10, 25 and 50 µg/mL of S2 is expressed in percentage and compared to the control cell group viability in Fig. 6. As observed from results obtained, both cells exhibited more than 80 % viability. Additionally, there was no significant difference in viability of cells between groups treated with different concentrations, thus can be concluded that S2 sample is non-cytotoxic in concentration up to 50 µg/mL. This agrees well with the determined viability of normal human gingival fibroblasts after incubation with α and β-$NaYF_4$:Yb, Er, nanoparticles synthetized under similar processing conditions [28,30].

To evaluate S2 potential for non-specific cell labeling, the lowest concentration of 10 µg/mL of UCNPs has been tested. HS-5 and SCC-25 were incubated for 24 h with S2 suspension, and laser scanning microscopy was performed afterward. As can be seen in Fig. 7, S2 UCNPs are located adjacent to the plasma membrane in the cytoplasmic region of both cell lines. All cells treated with S2 retained their distinctive morphology, as it is evidenced based on their auto-fluorescence under femtosecond laser excitation at 730 nm. The green fluorescent dots illustrate distribution of S2 UCNPs under excitation at 976 nm. Their positioning, obtained after overlapping of two former images, guarantees efficient cell labeling without compromising the integrity of the cell nucleus.

Taking into account that UCNPs possess temperature sensing capability due to the existence of thermally coupled levels (TCL) of doped activator ions, the intensity of radiative transitions originating from those levels changes in function of temperature. This occurs thanks to the fact that those levels have a small energy difference, so the higher level is thermally filled from the lower one following the Boltzmann population distribution rule. The *LIR* of spectral lines arising from the transitions from the TCL to the terminal level, as a function of absolute temperature, is:

$$LIR(T) = \frac{I_H(T)}{I_L(T)} = B^* e^{-\frac{\Delta E_{HL}}{kT}} \quad (1)$$

where $I_{H,L}$ are the luminescence intensities of the radiative transitions from the upper (H) and lower (L) TCL to the terminal level; ΔE_{HL} is the energy difference between H and L levels; k is the Boltzmann constant, and T is the absolute temperature. B is the temperature-invariant parameter, that belongs to the host material. The absolute and relative change of *LIR* in function of temperature indicates a material's potential to be used for sensing the temperature. The absolute sensitivity of the *LIR* to the temperature change is the partial derivative:

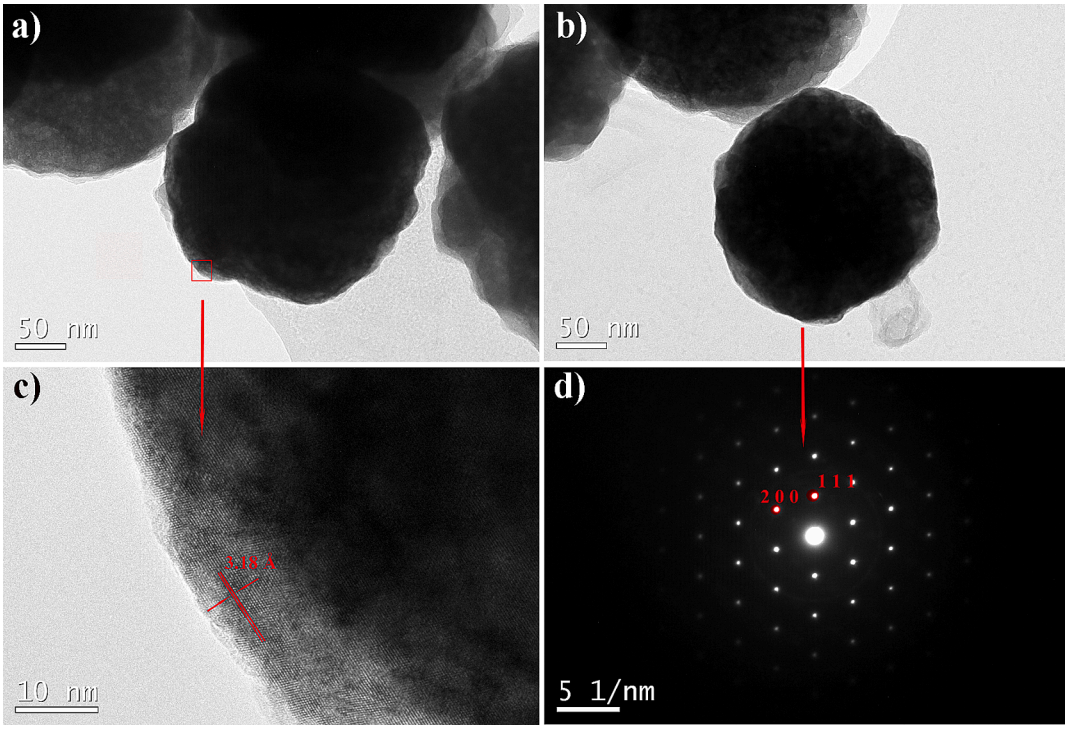

Fig. 3. TEM (a-c) and SAED pattern of S2 UCNPs.

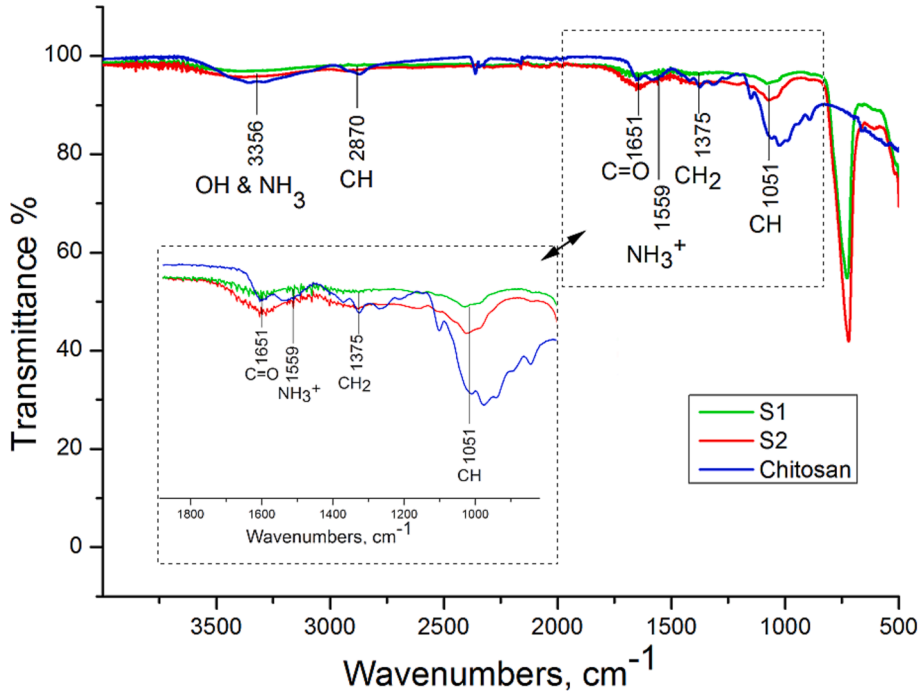

Fig. 4. FT-IR spectra of samples S1, S2 and pure chitosan. Inset shows magnified part where the chitosan-related ligands are visible in spectra of S1 and S2.

$$Sa = \left|\frac{\partial LIR}{\partial T}\right| = \frac{\Delta E_{HL}}{kT^2} * B * e^{-\frac{\Delta E_{HL}}{kT}} \quad (2)$$

The relative sensitivity is defined by:

$$Sr = \frac{Sa}{LIR} = \frac{\Delta E_{HL}}{kT^2} * 100\% \quad (3)$$

For Er^{3+}, TCL of interest are $^4S_{3/2}$ and $^2H_{11/2}$ levels and corresponding transitions to $^4I_{15/2}$ terminal level, which provoke appearance of the green emission. Fig. 8a reveals the change of the emission intensity with the rise of the temperature in the physiologically interesting temperature range from 20 °C to 65 °C. The anisotropic shape of wide emission peaks implies that their maxima cannot be simply read, and therefore a deconvolution needs to be done. The green emission spectra were fitted using six gaussian lines of similar spectral width (see Fig. S2) and their change with the temperature were examined. Change of the intensity of the green 523 nm ($^2H_{11/2} \rightarrow {}^4I_{15/2}$) and 539 nm ($^4S_{3/2} \rightarrow$

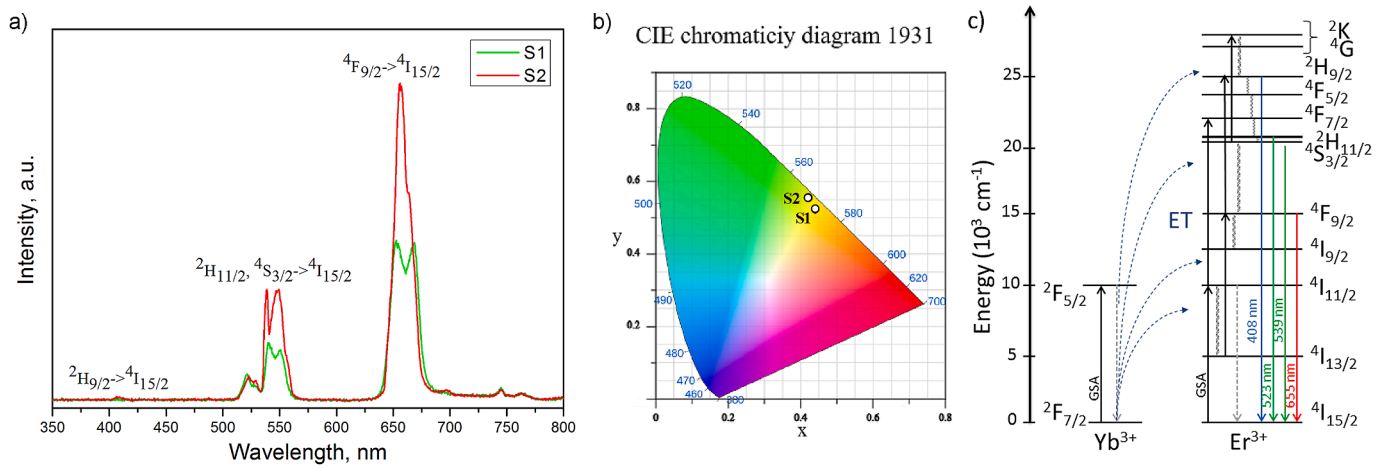

Fig. 5. Normalized UC emission spectra of S1 and S2, excited at 976 nm (a) with corresponding CIE 1931 diagram (b) and schematic energy diagram of Yb^{3+}/ Er^{3+} couple (c).

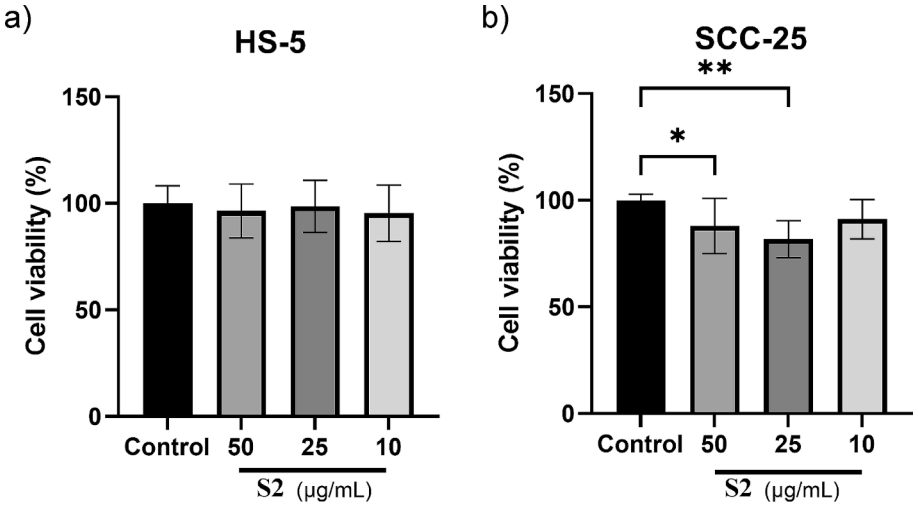

Fig. 6. Cytotoxicity assay of the sample S2 in HS-5 and SCC-25 after 24 h treatment. The data is shown as the mean ± SD (*P < 0.05, **P < 0.01 denote statistical significance).

$^4I_{15/2}$) emission in a function of temperature, is presented at Fig. 8b. It is notable that $^2H_{11/2} \rightarrow {}^4I_{15/2}$ radiative transition which is dependent of two competing processes, population through thermal excitation from $^4S_{3/2}$ level and depopulation through nonradiative $^4S_{3/2}$ level relaxation, changed negligible in investigated temperature range. Opposing to it, decreasing of 539 nm emission with the temperature increase was detected. As it was shown in [41], it is a consequence of enhancing the nonradiative relaxation to $^4F_{9/2}$ level, and thermal population of $^2H_{11/2}$ level. Such behavior of two emission lines is beneficial for ratiometric fluorescence temperature sensing. The corresponding LIR and the exponential line, fitted according to (1), are shown in Fig. 8c. Standard deviation for LIR of ± 0.0083, presented at Fig. 8c, was calculated based on ten consecutive measurements performed at 25 °C. This value does not change significantly at higher temperature, see Fig. S3.The fitted coefficient in the exponent in (1), equal to $-\Delta E_{HL}/k$, is 853 K, Fig. 8c. This value corresponds to the energy difference ΔE_{HL} of 0.0735 eV, which agrees very well with the theoretical value of $\Delta E_{HL} = 0.0704$ eV, calculated for the transition 523 nm → 539 nm. The absolute and relative sensitivities, calculated using the Eqs. (2) and (3) and experimentally obtained ΔE_{HL}, are presented in Fig. 8d. Fig. 8d shows that the absolute sensitivity (S_a) increases with increasing temperature. In contrast, the relative sensitivity (S_r) shows a quite opposite behaviour – its highest value of ~1.3 % K^{-1} is obtained at the lowest temperature. As can be seen from Table 2, S_r obtained in this work is comparable with the values reported for the most efficient βNaYF$_4$:Yb,Er,Gd phase (1.37 % K^{-1} [42]), and quite higher than of NaYF$_4$/Yb,Er@NaYF$_4$ core shell structures (1.1 % K^{-1} [43]), in the physiologically interesting temperature range.

4. Conclusions

Luminescent, biocompatible $NaY_{1-x}Gd_xF_4$:Yb/Er nanoparticles were obtained *in situ* by chitosan assisted solvothermal synthesis at 200 °C. The gadolinium introduction favors formation of α$NaY_{0.65}Gd_{0.15}F_4$:$Yb_{0.18}Er_{0.02}$ UCNPs with a stronger UC emission. The temperature dependent change in the green emission intensity, originating from the thermalization between $^4S_{3/2}$ and $^2H_{11/2}$ levels, was analyzed for possible thermometry applications in the physiologically interesting temperature range. The detected relative sensitivity of ~1.3 % K^{-1}, in combination with the excellent biocompatibility of UCNPs (cells viability greater than 80 %) and efficient HS-5 fibroblast and SCC-25 oral cancer cells visualization under NIR excitation, making them suitable for measuring of the temperature in tissues.

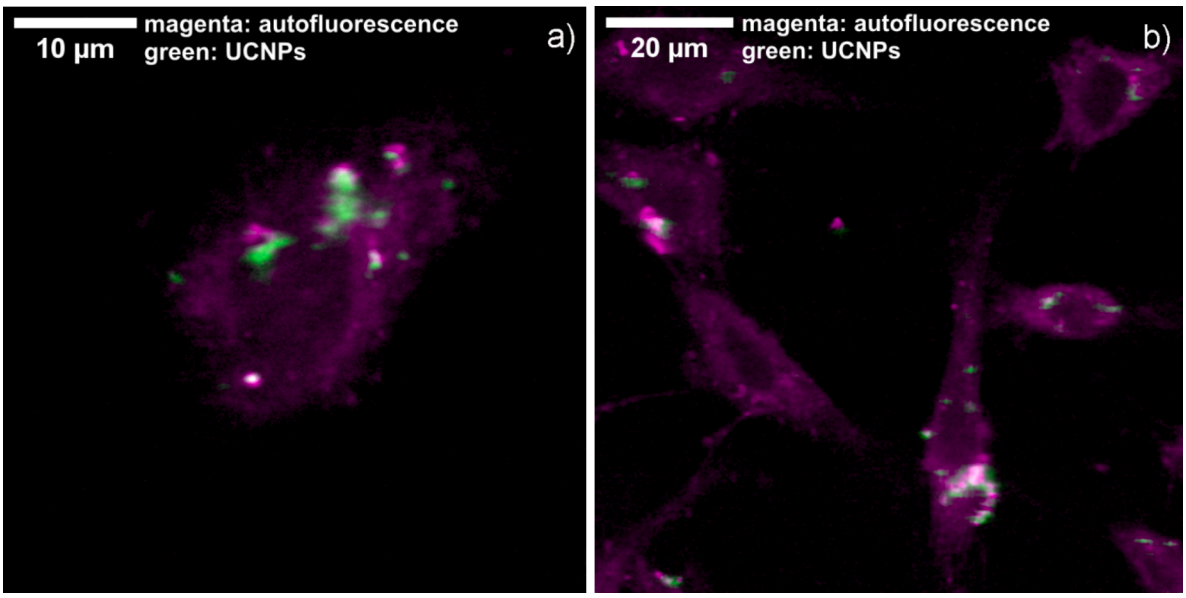

Fig. 7. Laser scanning microscopy images of SCC 25 and HS-5 cells incubated with 10 μg/mL of αNaY$_{0.65}$ Gd$_{0.15}$ F$_4$:Yb$_{0.18}$ Er$_{0.02}$ UCNPs.

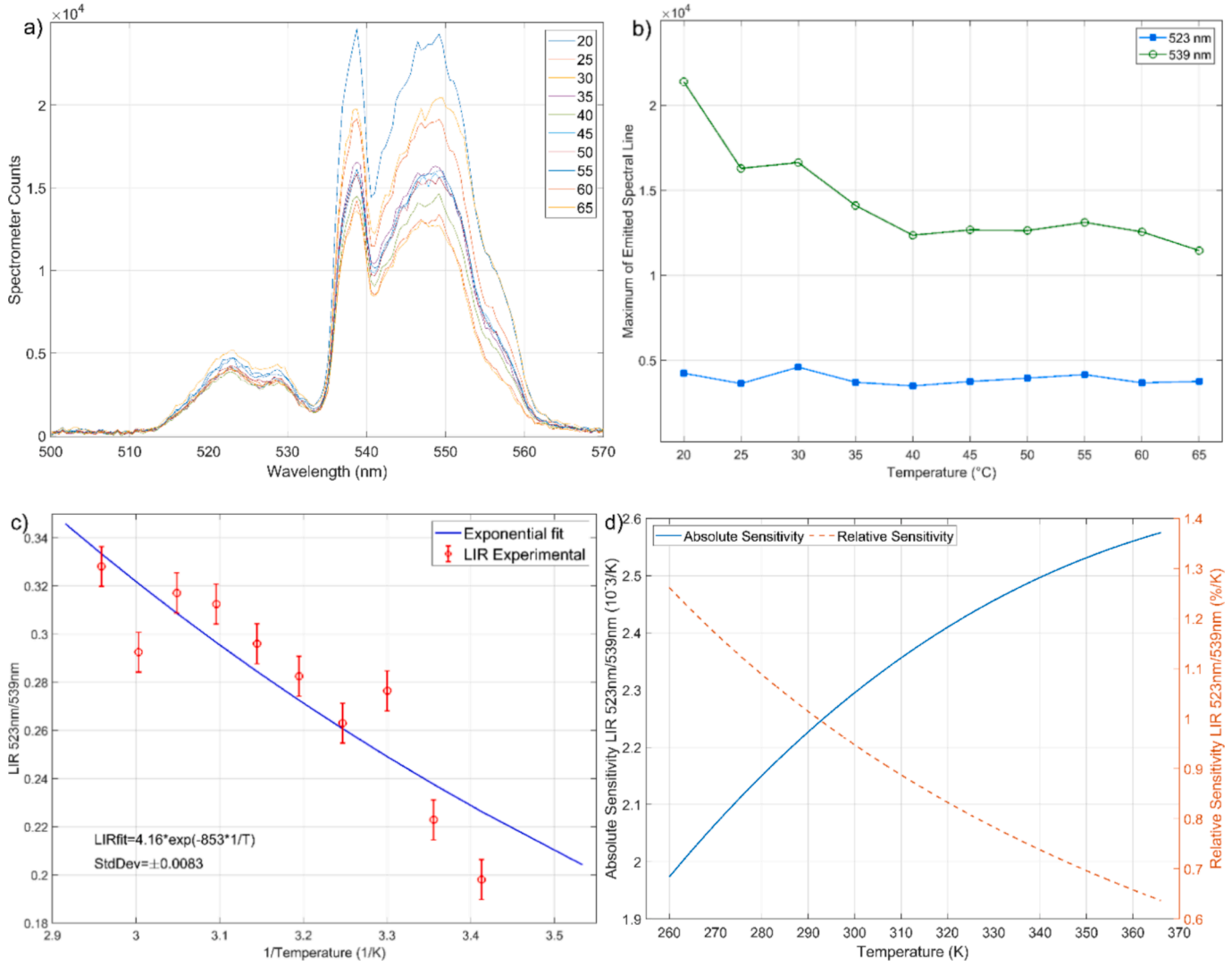

Fig. 8. Temperature-dependent UC emission spectra for green emission of αNaY$_{0.65}$Gd$_{0.15}$F$_4$:Yb$_{0.18}$Er$_{0.02}$ in the physiologically interesting temperature range (a), relative intensities of the 523 and 539 nm emissions as a function of temperature (b) *LIR* (c), and absolute and relative sensitivity (d).

Table 2
Sr values of other compounds reported for similar temperature range.

Compound	S_r ($\%K^{-1}$)	Temperature range (K)	Reference
$\alpha NaY_{0.65}Gd_{0.15}F_4$: $Yb_{0.18}Er_{0.02}$	1.3 at 260 K	533–633	This work
$\beta NaYF_4$:Yb,Er,Gd	1.37 at 288 K	285–325	[42]
$NaYF_4$/Yb,Er@$NaYF_4$	1.1 at 310 K	310–410	[43]
GdF_3:Yb,Er	0.53 at 310 K	300–330	[17]
$NaGdF_4$:Er^{3+}/Yb^{3+}	0.60 at 301 K	301–1173	[44]
$Ba_3Gd_2F_{12}$:Yb^{3+}/Er^{3+}	1.12 at 296 K	296–600	[16]
Sr_2InF_7:Yb,Er	1.4 at 300 K	200–450	[45]
YF_3:Yb,Er	1.2 at 300 K	273–373	[46]

CRediT authorship contribution statement

Miljana Piljević: Writing – original draft, Investigation. **Ivana Dinić:** Investigation, Conceptualization. **Lidija Mancic:** Writing – review & editing, Resources, Data curation. **Marina Vuković:** Validation, Formal analysis. **Miloš Tomić:** Visualization, Formal analysis, Data curation. **Maria Eugenia Rabanal:** Visualization, Formal analysis, Data curation. **Miloš Lazarević:** Visualization, Formal analysis, Data curation. **Mihailo D. Rabasović:** Supervision, Resources.

Declaration of competing interest

The authors declare that they have no known competing financial interests or personal relationships that could have appeared to influence the work reported in this paper.

Acknowledgments

The research was supported by the Ministry of Science, Technological Development and Innovation of the Republic of Serbia on the research programs of Institute of Physics Belgrade and Institute of Technical Sciences of SASA (Grant No. 451-03-136/2025-03/200175).

Appendix A. Supplementary material

Supplementary data to this article can be found online at https://doi.org/10.1016/j.inoche.2025.114239.

Data availability

Data will be made available on request.

References

[1] F. Auzel, Upconversion and anti-stokes processes with f and d ions in solids, Chem. Rev. 104 (2004) 139–173, https://doi.org/10.1021/cr020357g.
[2] Y. Li, C. Liu, P. Zhang, J. Huang, H. Ning, P. Xiao, Y. Hou, L. Jing, M. Gao, Doping lanthanide nanocrystals with non-lanthanide ions to simultaneously enhance up- and down-conversion luminescence, Front. Chem. 8 (2020) 832, https://doi.org/10.3389/fchem.2020.00832.
[3] J. Xie, W. Hu, D. Tian, Y. Wei, G. Zheng, L. Huang, E. Liang, Selective growth and upconversion photoluminescence of Y-based fluorides: from $NaYF_4$: Yb/Er to YF_3: Yb/Er crystals, Nanotechnology 31 (2020) 505605, https://doi.org/10.1088/1361-6528/abb627.
[4] M. Haase, H. Schäfer, Upconverting nanoparticles, Angew. Chem. Int. Ed. 50 (2011) 5808–5829, https://doi.org/10.1002/anie.201005159.
[5] S. Liu, G. De, X. Wang, Y. Xu, Y. Liu, J. Wanga, C. Cheng, A general strategy for the synthesis of rare earth fluoride nano(micro)crystals, CrstEngComm 20 (2018) 7293–7300, https://doi.org/10.1039/C8CE01296B.
[6] C. Li, J. Lin, Rare earth fluoride nano-/microcrystals: synthesis, surface modification and application, J. Mater. Chem. 20 (2010) 6831–6847, https://doi.org/10.1039/C0JM00031K.
[7] F. Wang, X. Liu, Recent advances in the chemistry of lanthanide - doped upconversion nanocrystals, Chem. Soc. Rev. 38 (2009) 976–989, https://doi.org/10.1039/B809132N.
[8] G. Murali, B. Hoon Lee, R.K. Mishra, J. Myeong Lee, S.-H. Nam, Y. Doug Suh, D.-K. Lim, J. Hee Lee, S. Hee Lee, Synthesis, luminescence properties, and growth mechanisms of YF_3:Yb^{3+}/Er^{3+} nanoplates, J. Mater. Chem. C 3 (2015) 10107–10113, https://doi.org/10.1039/C5TC02034D.
[9] Z. Fu, X. Cui, S. Cui, X. Qi, S. Zhou, S. Zhang, J. Hyun Jeong, Uniform Eu^{3+}-doped YF_3 microcrystals: inorganic salt-controlled synthesis and their luminescent properties, CrstEngComm 14 (2012) 3915–3922, https://doi.org/10.1039/C2CE00013J.
[10] J. Yu, W. Yin, T. Peng, Y. Chang, Y. Zu, J. Li, X. He, X. Ma, Z. Gu, Y. Zhao, Biodistribution, excretion, and toxicity of polyethyleneimine modified $NaYF_4$:Yb, Er upconversion nanoparticles in mice via different administration routes, Nanoscale 9 (2017) 4497–4507, https://doi.org/10.1039/C7NR00078B.
[11] W. Xu, L. Zhao, F. Shang, L. Zheng, Z. Zhang, Modulating the thermally coupled status of energy levels in rare earth ions for sensitive optical temperature sensing, J. Lumin. 249 (2022) 119042, https://doi.org/10.1016/j.jlumin.2022.119042.
[12] Z. Feng, L. Lin, Z. Wang, Z. Zheng, Highly efficient and wide range low temperature sensing of upconversion luminescence of $NaYF_4$: Er^{3+} nanoparticles: effects of concentration of active or sensitive ions, excitation power and particle size on temperature sensing sensitivity, Opt. Commun. 491 (2021) 126942, https://doi.org/10.1016/j.optcom.2021.126942.
[13] D. Chen, Z. Wan, Y. Zhou, P. Huang, J. Zhong, M. Ding, W. Xiang, X. Liang, Z. Ji, Bulk glass ceramics containing Yb^{3+}/Er^{3+}: β-$NaGdF_4$ nanocrystals: phase-separation-controlled crystallization, optical spectroscopy and upconverted temperature sensing behavior, J. Alloys Compd. 638 (2015) 21–28, https://doi.org/10.1016/j.jallcom.2015.02.170.
[14] J. Xi, M. Ding, M. Zhang, H. Zhang, D. Chen, Z. Ji, Monodispersed YF_3: Ce^{3+}/Tb^{3+}/Eu^{3+} mesocrystals: hydrothermal synthesis and optical temperature sensing behavior, J. Mater. Sci. Mater. Electron. 28 (2017) 9489–9494, https://doi.org/10.1007/s10854-017-6692-1.
[15] H. Hao, Z. Lu, H. Lu, G. Ao, Y. Song, Y. Wang, X. Zhang, Yb^{3+} concentration on emission color, thermal sensing and optical heater behavior of Er^{3+} doped $Y_6O_5F_8$ phosphor, Ceram. Int. 43 (2017) 10948–10954, https://doi.org/10.1016/j.ceramint.2017.05.133.
[16] L. Li, W. Wang, H. Chen, S. Li, Q. Zhang, Y. Pan, Y. Li, Optical thermometry based on upconversion luminescence of $Ba_3Gd_2F_{12}$: Yb^{3+}/Er^{3+} nanocrystals embedded in glass ceramics, J. Non Cryst. Solids 573 (2021) 121142, https://doi.org/10.1016/j.jnoncrysol.2021.121142.
[17] I. Dinić, M. Vuković, M.E. Rabanal, M. Milošević, M. Bukumira, N. Tomić, M. Tomić, L. Mančić, N. Ignjatović, Temperature sensing properties of biocompatible Yb/Er-Doped GdF_3 and YF_3 mesocrystals, J. Funct. Biomater. 15 (2024) 6, https://doi.org/10.3390/jfb15010006.
[18] A. Kumar, S. Prakash Tiwari, H.C. Swart, J.C. Gomes Esteves da Silva, Infrared interceded YF_3: Er^{3+}/Yb^{3+} upconversion phosphor for crime scene and anti-counterfeiting applications, Opt. Mater. 92 (2019) 347–351, https://doi.org/10.1016/j.optmat.2019.04.050.
[19] S. De Camillis, P. Ren, Y. Cao, M. Plöschner, D. Denkova, X. Zheng, Y. Lu, J. A. Piper, Controlling the non-linear emission of upconversion nanoparticles to enhance super-resolution imaging performance, Nanoscale 12 (2020) 20347–20355, https://doi.org/10.1039/D0NR04809G.
[20] J. Huang, L. Yan, S. Liu, N. Song, Q. Zhang, B. Zhou, Dynamic control of orthogonal upconversion in migratory core–shell nanostructure toward information security, Adv. Funct. Mater. 31 (2021) 2009796, https://doi.org/10.1002/adfm.202009796.
[21] T. Cao, T. Yang, Y. Gao, Y. Yang, H. Hu, F. Li, Water-soluble $NaYF_4$:Yb/Erupconversion nanophosphors: synthesis, characteristics and application in bioimaging, Inorg. Chem. Commun. 13 (2010) 392–394, https://doi.org/10.1016/j.inoche.2009.12.031.
[22] H. Ying Huang, A. Skripka, L. Zaroubi, B.L. Findlay, F. Vetrone, C. Skinner, J. Kwon Oh, L.A. Cuccia, Electrospun upconverting nanofibrous hybrids with smart NIR-light-controlled drug release for wound dressing, ACS Appl. Bio Mater. 3 (2020) 7219–7227, https://doi.org/10.1021/acsabm.0c01019.
[23] J. Xu, G. Du, C. Tong, S. Xie, H. Tan, L. Xu, N. Li, Controlled synthesis and panchromatic printing of highly luminescent $NaYF_4$:Ln^{3+} upconversion hollow microtubes for information encryption on various packaging substrates, J. Photochem. Photobiol. A Chem. 396 (2020) 112518, https://doi.org/10.1016/j.jphotochem.2020.112518.
[24] M.N.V.R. Kumar, A review of chitin and chitosan applications, React. Funct. Polym. 46 (2000) 1–27, https://doi.org/10.1016/S1381-5148(00)00038-9.
[25] F. Croisier, C. Jérôme, Chitosan-based biomaterials for tissue engineering, Eur. Polym. J. 49 (2013) 780–792, https://doi.org/10.1016/j.eurpolymj.2012.12.009.
[26] S. Gayathri, O. Sivaraman Nirmal Ghosh, A. Kasi Viswanath, P. Sudhakara, M. J. Kumar Reddy, A.M. Shanmugharaj, Synthesis of YF_3: Yb, Er upconverting nanofluorophores using chitosan and their cytotoxicity in MCF-7 cells, Int. J. Biol. Macromol. 72 (2015) 1308–1312, https://doi.org/10.1016/j.ijbiomac.2014.10.019.
[27] L. Gibot, S. Chabaud, S. Bouhout, S. Bolduc, F.A. Auger, V.J. Moulin, Anticancer properties of chitosan on human melanoma are cell line dependent, Int. J. Biol. Macromol. 72 (2015) 370–379, https://doi.org/10.1016/j.ijbiomac.2014.08.033.
[28] L. Mancic, A. Djukic-Vukovic, I. Dinic, M.G. Nikolic, M.D. Rabasovic, A.J. Krmpot, A.M.L.M. Costa, B.A. Marinkovic, L.J. Mojovic, O. Milosevic, One-step synthesis of amino-functionalized up-converting $NaYF_4$:Yb,Er nanoparticles for *in vitro* cell imaging, RSC Adv. 8 (2018) 27429–27437, https://doi.org/10.1039/C8RA04178D.

[29] TOPAS, General Profile and Structure Analysis Software for Powder Diffraction Data, V4.2; Bruker AXS GmbH, Karlsruhe, Germany, 2009.
[30] L. Mancic, A. Djukic-Vukovic, I. Dinic, M.G. Nikolic, M.D. Rabasovic, A.J. Krmpot, A.M.L.M. Costa, D. Trisic, M. Lazarevic, L.J. Mojovic, O. Milosevic, NIR photo-driven upconversion in $NaYF_4$:Yb,Er/PLGA particles for *in vitro* bioimaging of cancer cells, Mater. Sci. Eng. C 91 (2018) 597–605, https://doi.org/10.1016/j.msec.2018.05.081.
[31] K. Bukara, S.Z. Jovanic, I.T. Drvenica, A. Stancic, V. Ilic, M.D. Rabasovic, D. V. Pantelic, B.M. Jelenkovic, B. Bugarski, A.J. Krmpot, Mapping of hemoglobin in erythrocytes and erythrocyte ghosts using two photon excitation fluorescence microscopy, J. Biomed. Opt. 22 (2017) 026003, https://doi.org/10.1117/1.JBO.22.2.026003.
[32] I.A. Latif, H.M. Abdullah, M. Hameed Saleem, Electrical and swelling study of different prepared hydrogel, Am. J. Polym. Sci. 6 (2016) 50–57, https://doi.org/10.5923/j.ajps.20160602.04.
[33] S.M.L. Silva, C.R.C. Braga, M.V.L. Fook, C.M.O. Raposo, L.H. Carvalho, E. L. Canedo, Application of infrared spectroscopy to analysis of chitosan/clay nanocomposites, in: T. Theophanides (Ed.), Infrared Spectroscopy: Materials Science, Engineering and Technology, InTech, Rijeka, Croatia, 2012.
[34] Y. Yang, J. Cui, M. Zheng, C. Hu, S. Tan, Y. Xiao, Q. Yang, Y. Liu, One-step synthesis of amino-functionalized fluorescent carbon nanoparticles by hydrothermal carbonization of chitosan, Chem. Commun. 48 (2012) 380–382, https://doi.org/10.1039/C1CC15678K.
[35] S. Wang, A. Bi, W. Zeng, Z. Cheng, Upconversion nanocomposites for photo-based cancer theranostics, J. Mater. Chem. B 4 (2016) 5331–5348, https://doi.org/10.1039/C6TB00709K.
[36] H. Dong, L. Sun, C. Yan, Energy transfer in lanthanide upconversion studies for extended optical applications, Chem. Soc. Rev. 44 (2015) 1608–1634, https://doi.org/10.1039/C4CS00188E.
[37] M. Yuan, R. Wang, C. Zhang, Z. Yang, X. Yang, K. Han, J. Ye, H. Wang, X. Xu, Revisiting the enhanced red upconversion emission from a single β-$NaYF_4$:Yb/Er microcrystal by doping with Mn^{2+} ions, Nano Express 14 (2019) 103, https://doi.org/10.1186/s11671-019-2931-0.
[38] C.M.S. Calado, Í.F. Manali, I.M.S. Diogenis, S.F.N. Coelho, V.C. Teixeira, B.R. de Mesquita, J.L. Oliveira, F.A. Sigoli, M.V.S. Rezende, Defect disorder and optical spectroscopy study of Eu-doped $NaYF_4$ and $NaYGdF_4$ nanoparticles, Opt. Mater. 137 (2023) 113529, https://doi.org/10.1016/j.optmat.2023.113529.
[39] H. Yao, H. Shen, Q. Tang, C. Feng, Y. Li, Effect of Li co-doping with Er on up-conversion luminescence property and its temperature dependence of $NaY(WO_4)_2$, J. Phys. Chem. Solid 126 (2019) 189–195, https://doi.org/10.1016/j.jpcs.2018.11.009.
[40] A. Maurya, A. Bahadur, A. Dwivedi, A.K. Choudhary, T.P. Yadav, P. K. Vishwakarma, S.B. Rai, Optical properties of Er^{3+}, Yb^{3+} co-doped calcium zirconate phosphor and temperature sensing efficiency: effect of alkali ions (Li^+, Na^+ and K^+), J. Phys. Chem. Solid 119 (2018) 228–237, https://doi.org/10.1016/j.jpcs.2018.04.004.
[41] D. Gao, B. Chen, X. Sha, Y. Zhang, X. Chen, L. Wang, X. Zhang, J. Zhang, Y. Cao, Y. Wang, L. Li, X. Li, S. Xu, H. Yu, L. Cheng, Near infrared emissions from both high efficient quantum cutting (173%) and nearly-pure-color upconversion in $NaY(WO_4)_2$:Er^{3+}/Yb^{3+} with thermal management capability for silicon-based solar cells, Light Sci. Appl. 13 (2024) 17, https://doi.org/10.1038/s41377-023-01365-2.
[42] D.T. Klier, M.U. Kumke, Upconversion $NaYF_4$:Yb:Er nanoparticles co-doped with Gd^{3+} and Nd^{3+} for thermometry on the nanoscale, RSC Adv. 5 (2015) 67149–67156, https://doi.org/10.1039/C5RA11502G.
[43] S. Ye, L. Lei, Controlled synthesis of cubic $NaYF_4$:Yb/Er@$NaYF_4$ core/shell nanocrystals for ratiometric fluorescence temperature sensing, Chem. Phys. Lett. 833 (2023) 140935, https://doi.org/10.1016/j.cplett.2023.140935.
[44] A. Kumar, H. Couto, J.C.G.E. da Silva, Upconversion emission studies in Er^{3+}/Yb^{3+} doped/co-doped $NaGdF_4$ phosphor particles for intense cathodoluminescence and wide temperature-sensing applications, Materials 15 (2022) 6563, https://doi.org/10.3390/ma15196563.
[45] J. Tang, Y. Wu, M. Jin, Y. Li, C. Chen, J. Xiang, C. Guo, External-field-independent thermometric sensitivity and green emission of upconversion phosphor Sr_2InF_7:Yb^{3+}, Er^{3+}, Inorg. Chem. 61 (49) (2022) 20035–20042, https://doi.org/10.1021/acs.inorgchem.2c03379.
[46] A. Assy, H. Lin, M. Schoenauer-Sebag, P. Gredin, M. Mortier, L. Billot, Z. Chen, L. Aigouy, Nanoscale thermometry with fluorescent yttrium-based Er/Yb-doped fluoride nanocrystals, Sens. Actuators A: Phys., 250 (2016) 71–77, https://doi.org/10.1016/j.sna.2016.09.015.

Dr. Ivana Dinić, Senior Research Associate of ITS SASA, holds Ph.D in Biochemical engineering and biotechnology of Faculty of Technology and Metallurgy, University of Belgrade since 2019. She worked in Innovation Center of the Faculty of Chemistry until 2020, and she is currently employed in Institute of Technical Sciences of SASA. Her research interests are synthesis and characterization of hierarchical and hybrid optically active nanostructured materials with potential application in biomedicine, photocatalysis, environmental remediation, and solar cells. She published 15 scientific papers in SCI journals and 44 conference papers. Her ORCID number is 0000-0002-0909-8230.

University of Belgrade
Institute of Physics Belgrade
Kopaonik, March 10-14, 2024

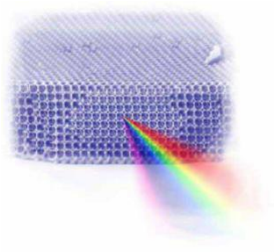

Book of Abstracts

17th Photonics Workshop

(Conference)

17th Photonics Workshop (2024)

Book of abstracts

Kopaonik, Serbia, March 10-14, 2024

Publisher, 2024:

Institute of Physics Belgrade

Pregrevica 118

11080 Belgrade, Serbia

Editors:

Dragan Lukić, Marina Lekić, Zoran Grujić

ISBN 978-86-82441-62-5

Printed by:

NEW IMAGE d.o.o.

Tošin Bunar 185, Belgrade

Number of copies: 60

CIP - Каталогизација у публикацији

Народна библиотека Србије, Београд

535(048)

681.7(048)

66.017/.018(048)

PHOTONICS Workshop (17 ; 2024 ; Kopaonik)

Book of Abstracts / 17th Photonics Workshop, (Conference), Kopaonik, March 10-14, 2024 ; [organized by Institute of Physics Belgrade, Photonics center [and] Optical Society of Serbia] ; [editors Dragan Lukić, Marina Lekić, Zoran Grujić]. - Belgrade : Institute of Physics, 2024 (Belgrade : New image). - 75 str. : ilustr. ; 25 cm

Tiraž 60. - Registar.

ISBN 978-86-82441-62-5

Selective in vitro labeling of cancer cells using NaGd0.8Yb0.17Er0.03F4 nanoparticles

Miljana Piljevic[1], Ivana Dinic[2], Marta Bukumira[1], Mihailo D. Rabasovic[1], Aleksandar J. Krmpot[1], Milos Lazarevic[3], and Lidija Mancic[2]

(1) *Photonic Center, Institute of Physics Belgrade, University of Belgrade, Pregrevica 118, Zemun, 11080, Belgrade, Serbia*

(2) *Institute of Technical Sciences of SASA, Kneza Mihaila St. 35, 11000, Belgrade, Serbia*

(3) *School of Dental Medicine, University of Belgrade, dr Subotica 8, 11000, Belgrade, Serbia*

Contact: Miljana Piljevic (miljana@ipb.ac.rs)

Abstract. Cancer represents one of the leading problems of today, with clinical detection oftentimes being difficult, currently based on imaging techniques, such as X-ray, computed tomography (CT) and magnetic resonance imaging (MRI). However, mortality rate is often reduced by early detection, therefore much focus has been directed towards developing methods for early detection of the disease. Recent research in the field of nanotechnology is focused on the use of nanoparticles, particularly Lanthanide-doped up-conversion nanoparticles (UCNPs), for the detection of cancer cells using near infrared (NIR) fluorescence microscopy. The reason for this is that in long-term tracking tests, near-infrared (NIR) light, has lower phototoxicity and higher tissue penetration depth in living systems as compared with UV/VIS light. In this research, $NaGd_{0.8}Yb_{0.17}Er_{0.03}F_4$ UCNPs were prepared by solvothermal synthesis in the presence of chitosan, a ligand which enables UCNPs biocompatibility and the specific antibody conjugation. Morphological and structural characterization of synthetized UCNPs were performed based on X-ray powder diffraction (XRPD), scanning electron microscopy (SEM), transmission electron microscopy (TEM), Fourier transform infrared spectroscopy (FTIR) and photoluminescence spectroscopy (PL). Results confirmed the presence of the cubic phase with a minor portion of hexagonal phase in nanoparticles. Synthesized nanoparticles were conjugated further with anti-human CD44 antibodies, labeled with fluorescein isothiocyanate (FITC), which signal is used for confirmation of nanoparticles positioning in cells. Such obtained conjugates were successfully used for selective *in vitro* biolabeling of oral squamous cell carcinoma cells.

TWENTY-SECOND YOUNG RESEARCHERS' CONFERENCE

MATERIALS SCIENCE AND ENGINEERING

December 4 – 6, 2024, Belgrade, Serbia

Program and the Book of Abstracts

Materials Research Society of Serbia
&
Institute of Technical Sciences of SASA

2024

Book title:
Twenty-Second Young Researchers' Conference - Materials Science and Engineering: Program and the Book of Abstracts

Publisher:
Institute of Technical Sciences of SASA
Kneza Mihaila 35/IV, 11000 Belgrade, Serbia
Tel: +381-11-2636994, 2185263, http://www.itn.sanu.ac.rs

Conference organizers:
Materials Research Society of Serbia, Belgrade, Serbia
Institute of Technical Sciences of SASA, Belgrade, Serbia

Editor:
Dr. Smilja Marković

Technical Editor:
Aleksandra Stojičić and Dr. Ivana Dinić

Cover page: Dr. Smilja Marković
Cover photo: Dr. Nebojša Labus

Printing:
Gama digital centar
Otona Župančića No. 19, 11070 Belgrade, Serbia
Tel: +381-63 8616734
http://www.gdc.rs

Publication year: 2024

Print-run:
120 copies

CIP - Каталогизација у публикацији

Народна библиотека Србије, Београд

66.017/.018(048)

YOUNG Researchers Conference Materials Sciences and Engineering (22 ; 2024 ; Beograd)
Program ; and the Book of abstracts / Twenty-Second Young Researchers' Conference Materials Science and Engineering, December 4 – 6, 2024, Belgrade, Serbia ; [organizers] Materials Research Society of Serbia & Institute of Technical Sciences of SASA ; [editor Smilja Marković]. - Belgrade : Institute of Technical Sciences of SASA, 2024 (Belgrade : Gama digital centar). - XXII, 89 str. ; 23 cm
Tiraž 120. - Registar.

ISBN 978-86-80321-39-4

a) Наука о материјалима -- Апстракти b) Технички материјали -- Апстракти
COBISS.SR-ID 157262345

Aim of the Conference

Main aim of the conference is to enable young researchers (post-graduate, master or doctoral student, or a PhD holder younger than 35) working in the field of materials science and engineering, to meet their colleagues and exchange experiences about their research.

Topics

Biomaterials
Environmental science
Materials for high-technology applications
Materials for new generation solar cells
Nanostructured materials
New synthesis and processing methods
Theoretical modelling of materials

Scientific and Organizing Committee

Milan Radovanović	Technical Faculty in Bor, Serbia
Vladimir Rajić	Institute of Nuclear Sciences "Vinča", Belgrade, Serbia
Julietta Rau	Institute of the Structure of Matter of the Italian National Research Council (ISM-CNR), Rome, Italy
Ana Stanković	Institute of Technical Sciences of SASA, Belgrade, Serbia
Boban Stojanović	Faculty of Sciences, Kragujevac, Serbia
Ivana Stojković Simatović	Faculty of Physical Chemistry, Belgrade, Serbia
Srečo Škapin	Institute Jožef Stefan, Ljubljana, Slovenia
Konrad Terpiłowski	Department of Interfacial Phenomena, Institute of Chemical Sciences, Faculty of Chemistry, Maria Curie-Skłodowska University in Lublin, Poland
Vuk Uskoković	TardigradeNano, Irvine, CA, USA
Rastko Vasilić	Faculty of Physics, Belgrade, Serbia
Ljiljana Veselinović	Institute of Technical Sciences of SASA, Belgrade, Serbia

Conference Secretary

Aleksandra Stojičić	Institute of Technical Sciences of SASA, Belgrade, Serbia

Conference Technical Committee

Katarina Aleksić, Marija Grujičić, Marko Jelić, Tamara Matić, Željko Mravik, Ana Nastasić, Milica Pejčić, Miljana Piljević, Jelena Rmuš-Mravik, Nina Tomić.

Results of the Conference

Beside printed «Program and the Book of Abstracts», which is disseminated to all conference participants, selected and awarded peer-reviewed papers will be published in journal "Tehnika – Novi Materijali". The best presented papers, suggested by Session Chairpersons and selected by Awards Committee, will be proclaimed at the Closing Ceremony. Part of the award is free-of-charge conference fee at YUCOMAT 2025.

Sponsors

Acknowledgement

The editor and the publisher of the Book of abstracts are grateful to the Ministry of Science, Technological Development and Innovation of the Republic of Serbia for its financial support of this book and The Twenty-Second Young Researchers' Conference - Materials Sciences and Engineering, held in Belgrade, Serbia.

2-6

Synthesis and characterization of $NaGd_{0.8}Yb_{0.17}Er_{0.03}F_4$ nanoparticles for selective *in vitro* labeling of cancer cells

Miljana Piljevic[1], Ivana Dinic[2], Marta Bukumira[1], Mihailo D. Rabasovic[1], Aleksandar J. Krmpot[1], Milos Lazarevic[3], Lidija Mancic[2]

[1]*Photonic Center, Institute of Physics Belgrade, University of Belgrade, Pregrevica 118, Zemun, 11080, Belgrade, Serbia*
[2]*Institute of Technical Sciences of SASA, Kneza Mihaila St. 35, 11000, Belgrade, Serbia*
[3]*School of Dental Medicine, University of Belgrade, dr Subotica 8, 11000, Belgrade, Serbia*

Lanthanide-doped up-conversion nanoparticles (UCNPs) represent a new class of contrast agents that show a significant potential in biomedical science for detection of cancer in early stages. These nanoparticles have the ability to emit visible or ultraviolet light upon excitation by near-infrared light, which enables noninvasive deep tissue imaging. This research presents synthesis of $NaGd_{0.8}Yb_{0.17}Er_{0.03}F_4$ UCNPs for selective labeling of oral squamous carcinoma cells. Nanoparticles were prepared through solvothermal synthesis in the presence of chitosan, a ligand which ensures UCNPs biocompatibility and enables further conjugation of selected antibodies. X-ray powder diffraction showed that majority of UCNPs crystallize in cubic structure, *s.g. Fm3m*, followed by low content of hexagonal-phased nanoparticles (~4 wt%). Scanning and transmission electron microscopy revealed that the obtained nanoparticles are cubic in shape and photoluminescence spectra indicated the double green emissions ($^2H_{11/2}$, $^4S_{3/2}\rightarrow{}^4I_{15/2}$) and a red emission ($^4F_{9/2}\rightarrow{}^4I_{15/2}$). Presence of protonated amino ligands at UCNPs surface, confirmed by Fourier transform infrared spectroscopy and X-ray photo spectroscopy, enabled UCNPs conjugation with anti-human CD44 antibodies (already labeled with fluorescein isothiocyanate - FITC), and their use for selective labeling of cancer cells. Commercially available SCC–25 (ATCC®, CRL–1628™) cancer cell line was used after magnetic-activated cell sorting of sub-populations of cells, $CD44^-$ and $CD44^+$. For the visualization of cells incubated with conjugated UCNPs, Nonlinear Laser Scanning Microscopy was used, with Ti:Sapphire laser as a light source, which operates in femto-second (fs) pulse mode or continuous wave (CW) mode; fs mode at 730 nm and at 800 nm was used for unlabeled cell imaging and the excitation of FITC respectively, while CW mode at 980 nm was used for the excitation of UCNPs. Upon 980 nm laser irradiation, it was shown that $NaGd_{0.8}Yb_{0.17}Er_{0.03}F_4$ UCNPs conjugated with CD44 antibodies were selectively attached only to $CD44^+$ sub-population of cells, while their presence was not detected on $CD44^-$ sub-population of cells. Since CD44 antigen has potential to identify tumorigenic cancer stem cells, using the UCNPs conjugated with anti-human CD44 antibodies enables detection of early-stage cancer.

Book of abstracts

PHOTONICA 2025

X International School and Conference on Photonics

25 - 29 August 2025

Belgrade, Serbia

Editors

Mihailo Rabasović, Uroš Ralević, Marina Lekić, Aleksandar Krmpot
Institute of Physics Belgrade, Serbia

Belgrade, 2025

ABSTRACTS OF TUTORIAL, KEYNOTE, INVITED LECTURES, PROGRESS REPORTS AND CONTRIBUTED PAPERS

of

X International School and Conference on Photonics
PHOTONICA 2025

25 - 29 August 2025

Belgrade, Serbia

Editors
Mihailo Rabasović, Uroš Ralević, Marina Lekić, Aleksandar Krmpot

Technical assistance
Stanko Nikolić and Marta Bukumira

ISBN 978-86-82441-72-4

Publisher
Institute of Physics Belgrade
Pregrevica 118
11080 Belgrade, Serbia

Printed by
Serbian Academy of Sciences and Arts, Knez Mihailova 35, Belgrade

Number of copies 30

CIP - Каталогизација у публикацији
Народна библиотека Србије, Београд
535(048)
621.37/.39:535(048)
621.37/.39:535]:61(048)
66.017/.018(048)
INTERNATIONAL School and Conference on Photonic (10 ; 2025 ; Beograd)
Book of abstracts / X International School and Conference on Photonics PHOTONICA 2025, 25 - 29 August 2025 Belgrade, Serbia ; editors Mihailo Rabasović ... [et al.]. - Belgrade: Institute of Physics, 2025 (Belgrade: SASA). - VIII, 175 str. : ilustr. ; 25 cm
Tiraž 30. - Bibliografija uz većinu apstrakata. - Registar.
ISBN 978-86-82441-72-4
1. Rabasović, Mihailo, 1977- [urednik]
a) Оптика -- Апстракти b) Оптички материјали -- Апстракти v) Оптоелектроника -- Апстракти g) Оптоелектроника -- Биомедицина -- Апстракти d) Телекомуникације -- Апстракти
COBISS.SR-ID 173823497

PHOTONICA 2025 (X International School and Conference on Photonics - www.photonica.ac.rs) is organized by Institute of Physics Belgrade, University of Belgrade (www.ipb.ac.rs), Serbian Academy of Sciences and Arts (www.sanu.ac.rs), and Optical Society of Serbia (www.ods.org.rs).

Other institution that helped the organization of this event are: Vinča Institute of Nuclear Sciences, University of Belgrade (www.vinca.rs), Faculty of Electrical Engineering, University of Belgrade (www.etf.bg.ac.rs), Institute of Chemistry, Technology and Metallurgy, University of Belgrade (www.ihtm.bg.ac.rs), Faculty of Technical Sciences, University of Novi Sad (www.ftn.uns.ac.rs), Faculty of Physics, University of Belgrade (www.ff.bg.ac.rs), and Faculty of Biology, University of Belgrade (www.bio.bg.ac.rs).

PHOTONICA 2025 is organized under auspices and with support of the Ministry of Science, Technological Development and Innovation, Serbia (https://nitra.gov.rs/en/).

The support of the sponsors of PHOTONICA 2025 is gratefully acknowledged:

Committees

Scientific Committee and Review Board

- Aleksandar Krmpot, Photonics center, Institute of Physics Belgrade, University of Belgrade, Serbia
- Aleksandra Maluckov, VINČA Institute of Nuclear Science, University of Belgrade, Serbia
- Bojan Resan, School of Engineering, FHNW University of Applied Sciences and Arts, Northwestern Switzerland
- Boris Malomed, Department of Physical Electronics, School of Electrical Engineering, Tel Aviv University, Israel
- Branislav Jelenković, Photonics center, Institute of Physics Belgrade, University of Belgrade, Serbia
- Carsten Ronning, Institute of Solid State Physics, Friedrich-Schiller-Universität Jena, Germany
- Concita Sibilia, Department of Basic and Applied Sciences for Engineering, Sapienza University of Rome, Italy
- Darko Zibar, Department of Photonics Engineering, Technical University of Denmark, Denmark
- Dmitry Budker, Johannes Gutenberg University Mainz, Germany, Germany
- Dragan Inđin, Institute of Microwaves and Photonics, School of Electronic and Electrical Engineering, University of Leeds, United Kingdom
- Edik Rafailov, Aston Institute of Photonic Technologies, School of Engineering and Applied Science, Aston University, United Kingdom
- Francesco Cataliotti, European Laboratory for Non-Linear Spectroscopy, University of Florence, Italy
- Giannis Zacharakis, Institute of Electronic Structure and Laser, Foundation for Research and Technology – Hellas, Greece
- Goran Isić, Institute of Physics Belgrade, University of Belgrade, Serbia
- Goran Mašanović, Optoelectronics Research Centre (ORC), Zepler Institute, Faculty of Engineering and Physical Sciences, University of Southampton, United Kingdom
- Ivana Vasić, Institute of Physics Belgrade, University of Belgrade, Serbia
- Jasna Crnjanski, School of Electrical Engineering, University of Belgrade, Serbia
- Jelena Radovanović, School of Electrical Engineering, University of Belgrade, Serbia
- Jelena Stašić, VINČA Institute of Nuclear Science, University of Belgrade, Serbia
- Jerker Widengren, Department of Applied Physics, Royal Institute of Technology, Stockholm, Sweden
- Jovan Bajić, Faculty of Technical Sciences, University of Novi Sad, Serbia
- Ljupčo Hadžievski, VINČA Institute of Nuclear Science, University of Belgrade, Serbia
- Luca Antonelli, Department of Physics, York Plasma Institute, University of York, United Kingdom
- Marco Canepari, Laboratoire Interdisciplinaire de Physique, Université Grenoble Alpes, France
- Marko Krstić, School of Electrical Engineering, University of Belgrade, Serbia
- Marko Spasenović, Institute of Chemistry, Technology, and Metallurgy, University of Belgrade, Serbia
- Milan Kovačević, Department of Physics, Faculty of Science, University of Kragujevac, Serbia

- Milena Milošević, The Centre for Laser Microscopy, Faculty of Biology, University of Belgrade, Serbia
- Milivoj Belić, Texas A&M University at Qatar, Qatar
- Mirjana Novaković, VINČA Institute of Nuclear Science, University of Belgrade, Serbia
- Nikola Stojanović, Deutsches Elektronen-Synchrotron DESY, Hamburg, Germany
- Nikola Vuković, School of Electrical Engineering, University of Belgrade, Serbia
- Nikos Pleros, Department of Informatics (CSD), Aristotle University of Thessaloniki, Greece
- Pavle Andjus, The Centre for Laser Microscopy, Faculty of Biology, University of Belgrade, Serbia
- Petra Beličev, VINČA Institute of Nuclear Science, University of Belgrade, Serbia
- Sergei Turitsyn, School of Engineering and Applied Science, Aston University, United Kingdom
- Vladan Pavlović, Department of Physics, University of Niš, Serbia
- Vladan Vuletić, MIT, United States of America
- Vladana Vukojević, Center for Molecular Medicine, Department of Clinical Neuroscience, Karolinska Institute, Stockholm, Sweden
- Zoran Grujić, Photonics center, Institute of Physics Belgrade, University of Belgrade, Serbia

Organizing Committee

- Marina Lekić, Institute of Physics Belgrade (Chair)
- Aleksandar Krmpot, Institute of Physics Belgrade (Co-Chair)
- Uroš Ralević, Institute of Physics Belgrade (Co-Chair)
- Dušica Vukčević Stojiljković, Institute of Physics Belgrade (Secretary)
- Stanko Nikolić, Institute of Physics Belgrade (Webmaster)
- Mihailo Rabasović, Institute of Physics Belgrade
- Marija Ćurčić, Institute of Physics Belgrade
- Marta Bukumira, Institute of Physics Belgrade
- Miljana Piljević, Institute of Physics Belgrade
- Milica Ćurčić, Institute of Physics Belgrade
- Branka Hadžić, Institute of Physics Belgrade
- Aleksandra Kocić, Institute of Physics Belgrade
- Bojana Bokić, Institute of Physics Belgrade

Technical Organizer

Lufthansa City Center
Panacomp Wonderland
Travel

http://www.panacomp.net/
Tel: +381 21 466 075
Tel: +381 21 466 076
Tel: +381 21 466 077

Nonlinear Laser Scanning Microscopy for noninvasive imaging of cells labeled by up-converting $NaY_{0.65}Gd_{0.15}F_4:Yb_{0.18}Er_{0.2}$ nanoparticles

M. Piljević[1], I. Dinić[2], L. Mancic[2], M. Vuković[2], M. Tomić[2], M. E. Rabanal[3], M. Lazarević[4], M. D. Rabasović[1]

[1]*Photonic Center, Institute of Physics Belgrade, University of Belgrade, Pregrevica 118, Zemun, 11080, Belgrade, Serbia*

[2]*Institute of Technical Sciences of SASA, Kneza Mihaila St. 35, 11000, Belgrade, Serbia*

[3]*Department of Materials Science and Engineering and Chemical Engineering, Universidad Carlos III de Madrid and IAAB, 28903, Madrid, Spain*

[4]*School of Dental Medicine, University of Belgrade, dr Subotica 8, 11000, Belgrade, Serbia*

e-mail: miljana@ipb.ac.rs

Nonlinear Laser Scanning Microscopy (NLSM) is a modern technique that utilizes ultrafast-pulsed lasers in the near-infrared wavelength range, which makes it suitable for noninvasive imaging of living cells. In this study, $\alpha NaY_{0.65}Gd_{0.15}F_4:Yb_{0.18}Er_{0.2}$ nanoparticles were synthetized and their potential for non-specific cell labeling was investigated using NLSM. These up-converting nanoparticles (UCNPs) have a significant potential in biomedical sciences as fluorescent probes for early cancer detection. Upon excitation by near-infrared light UCNPs are able to emit visible or ultraviolet photons, enabling deep noninvasive tissue imaging. The solvothermal synthesis applied chitosan, a polymer that ensures biocompatibility of synthetized UCNPs. Their morphological and structural characterization included following analyses: X-ray powder diffraction, scanning electron microscopy coupled with energy-dispersive X-ray spectroscopy, transmission electron microscopy, Fourier transform infrared spectroscopy and photoluminescence spectroscopy. Cell lines tested for labeling and visualization were HS-5 fibroblast healthy cells and SCC–25 oral cancer cells. Following nanoparticles incubation in these, NLSM was performed using Ti:Sapphire laser (Coherent, Mira 900-F) as a laser light source, operating in both, femto-second pulse mode and continuous wave mode. In order to visualize cells through their autofluorescence, excitation wavelength of 730 nm in femtosecond mode was used, while for their visualization through excitation of incubated nanoparticles continuous wavelength of 976 nm was used. Obtained images implied that the UCNPs were located adjacent to the plasma membrane in the cytoplasmic region of both healthy and cancer cells, without disturbing the morphology of cells. Besides this, UCNPs exhibited relative temperature sensitivity of ~1.3% K^{-1} indicating their potential for measuring the temperature in tissues.

ORCID: M.P. 0000-0002-6367-8316, I.D. 0000-0002-0909-8230, L.M. 0000-0002-6620-9582, M.V. 0000-0001-5824-3484, M.T. 0000-0003-1436-2208, M.E.R. 0000-0002-5090-6498, M.L. 0000-0003-1330-5332, M.D.R. 0000-0002-9235-4388

TWENTY-SIXTH ANNUAL CONFERENCE ON MATERIAL SCIENCE

YUCOMAT 2025

Hunguest Hotel Sun Resort, Herceg Novi, Montenegro
September 1 to 5, 2025

Program
and
Book of Abstracts

Organised by
Materials Research Society of Serbia

Endorsed by
Federation of European Material Societies

CIP - Каталогизација у публикацији
Народна библиотека Србије, Београд

66.017/.018(048)
621.762.5(048)

DRUŠTVO za istraživanje materijala Srbije (Beograd). Godišnja konferencija (26 ; 2025 ; Herceg Novi)
Programme ; and The Book of Abstracts / Twenty-sixth Annual Conference YUCOMAT 2025, Herceg Novi, Montenegro, September 1-5, 2025 ; organised by Materials Research Society of Serbia ; [editor Dragan P. Uskoković]. - Belgrade : Materials Research Society of Serbia, 2025 (Herceg Novi : Biro Konto). - XXXVIII, 142 str. : ilustr. ; 24 cm

Tiraž 200. - Bibliografija uz pojedine apstrakte. - Registar.

ISBN 978-86-919111-8-8 (broš.)

a) Наука о материјалима -- Апстракти b) Технички материјали -- Апстракти v) Наноматеријали -- Апстракти

COBISS.SR-ID 173754377

26th ANNUAL CONFERENCE ON MATERIAL SCIENCE **YUCOMAT 2025**
Herceg Novi, Montenegro, September 1 to 5, 2024

Program and Book of Abstracts

Publisher: Materials Research Society of Serbia
Knez Mihailova 35/IV, P. O. Box 433, 11000 Belgrade, Serbia
Phone: +381 11 2185-437; http://www.mrs-serbia.org.rs

Editor: Prof. Dr. Dragan P. Uskoković

Conference Secretary: Jasmina Jevtić and Miljana Jovanović

Technical editors: Dr. Ivana Dinić

Typesetting and prepress: Dr. Aleksandar Dekanski

Covers: Front cover photo: property of MRS Serbia
Back cover photo: Marcin Konsek / Wikimedia Commons - CC BY-SA 4.0

ISBN 978-86-919111-8-8
https://doi.org/10.5281/zenodo.16887515

MRSS is member of the Federation of European Materials Societies

Printed in: **Biro Konto**, Sutorina bb, Igalo - Herceg Novi, Montenegro
Phones: +382-31-670123, 670025, E-mail: bkonto@t-com.me

Circulation: 200 copies. The end of printing: August 2025

P.S.63.

Targeting cancer cells by up-converting $NaGd_{0.8}Yb_{0.17}Er_{0.03}F_4$ nanoparticles

Ivana Dinić[1], Miljana Piljević[2], Marina Vuković[1], Marta Bukumira[2], Mihailo D. Rabasović[2], Miloš Lazarević[3], Lidija Mančić[1]

[1]*Institute of Technical Sciences of SASA, Belgrade, Serbia*
[2]*Photonic Center, Institute of Physics Belgrade, University of Belgrade, Serbia*
[3]*Institute of Human Genetics, School of Dental Medicine, University of Belgrade, Serbia*

In current medical research, biological imaging holds an important position in diagnostics, as it allows visualization of cell morphology and the processes occurring within them. As a result, considerable attention has been directed towards the development of novel types of biomarkers, including up-converting nanoparticles (UCNP) optically active under near-infrared (NIR) radiation. Lanthanide-doped UCNPs offer advantages over currently used fluorophores, due to the absence of tissue autofluorescence, minimized local heating, non-bleaching, and stable response. In this work, biocompatible $NaGd_{0.8}Yb_{0.17}Er_{0.03}F_4$ UCNPs nanoparticles were synthesized through one-pot solvothermal processing with assistance of chitosan. Obtained nanoparticles were analyzed by X-ray powder diffraction (XRPD), field emission scanning electron microscopy (FE-SEM), transmission electron microscopy (TEM), Fourier transform infrared (FTIR) and photoluminescence (PL) spectroscopy. The findings confirmed crystallization of the cubic crystals with a good luminescence response. To assess the biological safety of their use, a cytotoxicity test was conducted. Additionally, nanoparticles were conjugated with anti-human CD44 antibodies labeled with fluorescein isothiocyanate (FITC) and incubated with HS-5 fibroblasts and oral squamous cell carcinoma OSCC cells. Scanning laser microscopy is used for *in vitro* imaging of labeled cells. Based on the colocation of the FITC and UCNPs signals, selective labeling of OSCC cells was verified.